

Temperature-Dependent Dynamic Mechanical Analysis–Fourier Transform Infrared Study of a Poly(ester urethane) Copolymer

Haochuan Wang,[†] Steven R. Aubuchon,[‡] Darla Graff Thompson,[§] Jill C. Osborn,[§] Anderson L. Marsh,[§] William R. Nichols,[§] Jon R. Schoonover,[§] and Richard A. Palmer^{*,†}

Department of Chemistry, Duke University, Box 90346, Durham, North Carolina 27708-0346; TA Instruments Inc., 109 Lukens Drive, New Castle, Delaware 19720; and Materials Science and Technology Division, MS E549, Los Alamos National Laboratory, Los Alamos, New Mexico 87545

Received December 10, 2001

ABSTRACT: Variable temperature dynamic mechanical analysis (DMA) and Fourier transform infrared spectroscopy (FTIR) have been combined and applied to rheo-optical (DMA-FTIR) studies of thin films of a poly(ester urethane). In this study, dynamic infrared linear dichroism (DIRLD) measurements have been carried out at 25, –5, and –30 °C with the step-scan FTIR modulation/demodulation technique. The changes in both the in-phase and quadrature spectra as a function of temperature reveal different responses for the various functional groups as a function of temperature. In particular, as the temperature is lowered, the dynamic responses of structurally different carbonyl groups (hydrogen-bonded, free, urethane, ester) are clearly differentiated. The changes in dynamic response are related to changes in the hydrogen-bonding interactions in this polymer as well as to distinction between different molecular-level microenvironments.

Introduction

Thermoplastic elastomers derive their mechanical properties from the thermodynamic incompatibility between flexible soft segments and covalently attached hard segments. Molecular-level effects fundamentally determine the macroscopic properties of these materials, which are the basis of their various uses. There is, therefore, considerable interest in the use of experimental probes capable of monitoring molecular-level structure and orientation.

Poly(ester urethanes) represent one group of elastomers where the phase separation of the polyurethane segments into domains greatly increases the modulus and strength. The poly(ester urethane) used in this study is a segmented polymer obtained by polymerization of 4,4'-diphenylmethane diisocyanate and polybutylene adipate with 1,4-butanediol. The polyurethane segments associate with one another to form hard domains that act as physical cross-links between the polyester soft segments. The hard segments include hydrogen bonds between the carbonyl and N–H groups of the urethane groups. The N–H groups can also hydrogen bond to the polyester carbonyl and ether oxygens. These hard and soft domains and the associated hydrogen-bonding interactions help to provide the distinctive elastomeric, thermal, and mechanical properties of this material and account for its usefulness in a wide range of applications.

Infrared (IR) spectroscopy is especially suited for obtaining molecular-level structural and orientational information on this type of segmented polymer. The infrared approach is capable of differentiating between hard and soft domain vibrations as well as the vibra-

tions associated with hydrogen-bonding interactions. Since molecular-level effects determine the macroscopic mechanical properties, the specificity of the IR experiment makes it an attractive approach to study structure–property relationships.^{1,2} The mechanical responses of viscoelastic materials are time-dependent and require the use of dynamic measurement methods such as dynamic mechanical analysis (DMA).³ In previous (ambient temperature) investigations, DMA and dynamic Fourier transform infrared (FTIR) spectroscopy have been interfaced so that both DMA and dynamic infrared characterization could be carried out simultaneously (DMA–FTIR or infrared optorheology).¹ While the DMA provides macroscopic viscoelastic parameters, the dynamic infrared linear dichroism (DIRLD) experiment monitors the orientation dynamics of the macromolecular chains and organic functional groups, thus providing a combination of macroscopic and microscopic rheological characterization.

In the pioneering work of Noda, the DMA was set in the small-amplitude sinusoidal deformation mode, and initial DIRLD experiments were performed using a dispersive infrared spectrometer.^{4,5} More recently, the introduction of step-scan FTIR has provided a more effective method for phase-resolved infrared spectral detection over a broad spectral range.^{6–8} The step-scan mode of FTIR spectrometers is now the primary method for DIRLD measurements, enabling the study of dynamic stress-induced reorientation on the molecular and sub-molecular scale with sub-millisecond time resolution.^{9–15}

Previous DMA–FTIR experiments have supplied insight into the effect of added plasticizer and hydrolytic degradation on the poly(ester urethane) used in this study.^{15,16} However, the infrared spectrum and the DIRLD responses are complex, with numerous overlapping bands. Furthermore, at ambient temperature, it is difficult to differentiate polyester (soft) and polyurethane (hard) segment responses since most of the

[†] Duke University.

[‡] TA Instruments.

[§] Los Alamos National Laboratory.

* Corresponding author: e-mail richard.a.palmer@duke.edu; phone (919)-660-1605; Fax (919)-660-1605.

measured responses tend to be in-phase with the oscillating deformation under these experimental conditions.

However, characteristic of viscoelastic materials, organic polymers have significantly retarded rheological responses near their glass transition temperatures (T_g). Thus, variable temperature DMA/DIRLD measurements have the potential to supply additional insight into structure–function relationships, since the numerous overlapping features may be distinguished due to different reorientation responses, to applied strain near T_g . In this paper, we present the results of an investigation of dynamic reorientation effects as the temperature is lowered to the vicinity of the polyester (soft segment) glass transition.

Experimental Section

Sample Preparation. The polymer of interest in the current study is Estane 5703 (hereafter referred to as Estane), which serves as the binder in high explosive formulations as well as in numerous other industrial and consumer applications. Thin films of Estane, poly(butylene adipate)–poly-(4,4'-diphenylmethane diisocyanate-1,4-butanediol) (B.F. Goodrich), were prepared by solvent casting from a methylethyl ketone solution at a concentration of 15 wt %.¹⁶ The solution was poured over a Teflon film or onto optical quality BaF₂ plates. After solvent evaporation, the films were further dried in an oven at 60 °C and atmospheric pressure for 2–3 days. Free-standing films were peeled off the Teflon support, cut to size, and mounted in either the DMA or the Polymer Modulator. These samples were prestretched to 500–600% strain prior to the dynamic IR studies. Static IR measurements were made directly on the samples cast on BaF₂ windows or prestretched samples sandwiched between two windows.

Differential Scanning Calorimetry (DSC). DSC analysis was carried out using a TA Instruments modulated DSC model 2980 (TA Instruments, New Castle, DE) on a solvent-cast sample. The DSC data were measured by scanning the temperature from –70 to +120 °C with a temperature incremental rate of 2 °C/min. Heat flow in to and out of the Estane sample was measured as the sample temperature increased.

Variable Temperature Static Infrared Measurements. Variable low-temperature, static FTIR measurements (0 to –30 °C) were made using a Perkin-Elmer 1760X spectrometer equipped with a MCT detector. The polymer sample cast on a BaF₂ plate was cooled using an APD Cryogenics HC-2 cryostat. Static FTIR measurements were also made at ambient temperature.

Dynamic Mechanical Analysis (DMA). DMA was performed on a piece of Estane film cut and mounted between the tensile mode clamps of the instrument. The sample was prestretched about 500% to be similar to the samples used in the DIRLD studies. The dimensions of the film were approximately 10 mm long by 7.5 mm wide by 0.02 mm thick. A sinusoidal small-amplitude (ca. 50 μ m) deformation of 20 Hz was applied during a temperature sweep from –55 to +55 °C at a rate of 3 °C/min.

Variable Temperature DMA–FTIR Measurement. Dynamic FTIR experiments were performed with a Bruker Optics IFS66/s spectrometer equipped with an MCT detector. The spectrometer was operated in the step-scan mode using its internal digital signal processing (DSP) function for demodulation in the phase-resolved dynamic measurements. The Polymer Modulator (PM, Manning Applied Technology) has been used previously but was modified in this study for limited variable temperature operation.^{15,16} The two open sides of the PM were closed with plates of poly(methyl methacrylate), with each of the two plates possessing a 25 mm KBr window in the middle. The two windows and one of the two plastic plates can be easily removed to allow for sampling changing. The stainless steel frame of the PM and the two plastic plates form a small compartment with the polymer film held by the two

Table 1. Estane FTIR Band Assignments (3400–1000 cm^{–1}) and Domain Origin (Hard = Polyurethane, Soft = Polyester)

| IR band (cm ^{–1}) | assignment | domain origin |
|-----------------------------|---------------------------------------------|---------------|
| 3343 | ν (N–H) | hard |
| 2957 | ν (C–H) | hard/soft |
| 2923 | ν (C–H) | hard/soft |
| 2875 | ν (C–H) | hard/soft |
| 1732 | ν (C=O) | hard/soft |
| 1610, 1597 | phenyl ring 8a, 8b | hard |
| 1533 | ν (C–N) + δ (N–H) | hard |
| 1464 | CH ₂ deformation | soft |
| 1415 | phenyl ring 19b | hard |
| 1394, 1362 | CH ₂ wag | soft |
| 1311 | ν (C–N) + δ (N–H), phenyl ring 3 | hard |
| 1256 | ν (C–O–C), (CH ₂) wag | soft |
| 1223 | ν (C–N) + δ (N–H) | hard |
| 1207 | phenyl ring | hard |
| 1174 | ν (C–O–C) | soft |
| 1143 | CH ₂ vibration | soft |
| 1074 | ν (C–O–C) | hard/soft |
| 1019 | phenyl ring 18a | hard |

jaws, enclosed. To further improve the heat insulation efficiency of this small compartment, the outside of the frame of the PM was covered with several layers of aluminized Mylar film. A J-type thermocouple was used for monitoring the temperature near the sample film.

Two thick-wall Tygon tubes are connected to the inside of the sealed PM to allow dry air to circulate in and out. The dry air was generated by the same Balston air-dryer used to supply air for the interferometer air bearing and spectrometer purge. For subambient operation, a homemade temperature control module directs part of the dry air supply through a copper coil immersed in a temperature-controlled bath (in these studies, a bath of 2-propanol and dry ice slurry; ca. –60 °C). This air is then directed through the PM. For the current experiment, electronic feedback control of the PM temperature was not available; the temperature was manually controlled by the operator by varying the dry air flow rate. Temperature stability was determined to be ca. ± 1 °C.

DIRLD measurements were performed at room temperature (25 °C), –5 °C, and –30 °C. The room temperature DIRLD data have been reported on previously.^{15,16} The previous room temperature measurements were performed by use of a ZnSe photoelastic modulator (PEM) to create polarization modulation. To take advantage of the internal DSP function of the spectrometer and to eliminate the use of a high-frequency lock-in amplifier (for demodulating the polarization modulation of the PEM), the DIRLD measurements in the study reported here were performed without a PEM, using only a wire grid linear polarizer. Two dynamic measurements were required: one with the linear polarizer in the parallel orientation (relative to the strain direction) and one with the polarizer in the perpendicular orientation. Then, the static and dynamic absorptions in both polarizations were calculated. Subtraction of the data measured from the two polarizations provides the static and dynamic dichroic difference spectra. Comparison of results with and without the PEM demonstrates that the PEM method and the polarizer method for DIRLD measurements yield equivalent results.

Results

FTIR Spectrum. The FTIR spectrum of Estane has been discussed previously.^{15,16} Band assignments for the mid-infrared fingerprint region (3400–1000 cm^{–1}) are listed in Table 1. Bands that are associated either with the phenyl ring or the urethane functional groups are classified as hard segment bands. Phenyl ring modes are identified in Table 1 using Wilson's vibrational number for benzene. Soft segment bands are primarily associated with motions of the –CH₂– functional groups

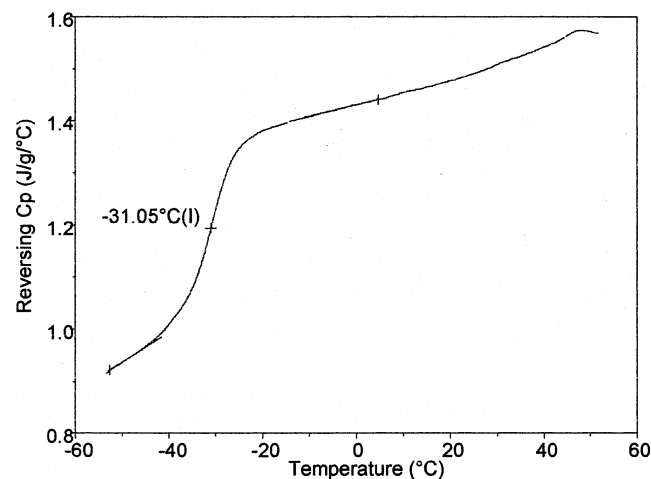


Figure 1. Differential scanning calorimetry (DSC) data for solvent cast thin film of the poly(ester urethane) referred to as Estane.

or the $\nu(\text{C}-\text{O}-\text{C})$ vibrations of the ester groups. Bands that have contributions from both segments are so labeled; these bands include the carbonyl band at 1732 cm^{-1} , the $\nu(\text{C}-\text{O}-\text{C})$ band at 1074 cm^{-1} , and the $\nu(\text{C}-\text{H})$ features ($3100\text{--}2800\text{ cm}^{-1}$). With the considerable overlap in the carbonyl region, it is difficult to use this region of the spectrum to supply information on the two domains.

Differential Scanning Calorimetry (DSC). Differential scanning calorimetry was performed to understand the thermal behavior of the unoriented, solvent-cast film of Estane. The DSC data are shown in Figure 1. A glass transition is indicated near $-30\text{ }^{\circ}\text{C}$, and an endothermic transition between 40 and $60\text{ }^{\circ}\text{C}$ is also observed. The T_g near $-30\text{ }^{\circ}\text{C}$ corresponds to the glass transition temperature of the polyester soft domains, while the endothermic transition is associated with disruption of the polyurethane hard domain network structure.

Variable Low-Temperature Static Infrared Measurements. Static FTIR difference spectra as a function

Table 2. Difference Features Observed in the Temperature-Dependent Difference Spectrum

| band, cm^{-1} | assignment | domain origin |
|------------------------|--------------------------------------------------------------------------------|---------------|
| 1741 | $\nu(\text{C}=\text{O})$, free ester and urethane | hard/soft |
| 1726 | $\nu(\text{C}=\text{O})$, H-bonded ester | soft |
| 1705 | $\nu(\text{C}=\text{O})$, H-bonded urethane | hard |
| 1610 | phenyl ring 8a | hard |
| 1597 | phenyl ring 8b + $\delta(\text{N}-\text{H})$, H-bonded | hard |
| 1593 | phenyl ring 8b + $\delta(\text{N}-\text{H})$, free | hard |
| 1540 | $\nu(\text{C}-\text{N})$ + $\delta(\text{N}-\text{H})$, H-bonded | hard |
| 1525 | $\nu(\text{C}-\text{N})$ + $\delta(\text{N}-\text{H})$, free | hard |
| 1316 | $\nu(\text{C}-\text{N})$ + $\delta(\text{N}-\text{H})$ H-bonded, phenyl ring 3 | hard |
| 1303 | $\nu(\text{C}-\text{N})$ + $\delta(\text{N}-\text{H})$ free | hard |
| 1256 | $\nu(\text{C}-\text{O}-\text{C})$, (CH_2) wag | soft |
| 1228 | $\nu(\text{C}-\text{N})$ + $\delta(\text{N}-\text{H})$ H-bonded | hard |
| 1217 | $\nu(\text{C}-\text{N})$ + $\delta(\text{N}-\text{H})$ free | hard |
| 1174 | $\nu(\text{C}-\text{O}-\text{C})$ H-bonded | soft |
| 1152 | $\nu(\text{C}-\text{O}-\text{C})$ free | soft |
| 1080 | $\nu(\text{C}-\text{O}-\text{C})$ H-bonded | hard/soft |
| 1057 | $\nu(\text{C}-\text{O}-\text{C})$ free | hard/soft |

of temperature of an unoriented solvent-cast film are shown in Figure 2. The spectra were measured at 0 , -6 , -12 , -18 , -24 , and $-30\text{ }^{\circ}\text{C}$. The room temperature spectra have been subtracted from each of these to produce the difference spectra. These data are used to help identify the different hydrogen-bonding components of the infrared bands. The difference spectra demonstrate primarily the differences in hydrogen-bonded and non-hydrogen-bonded components for functional groups that act as hydrogen-bonding donors or acceptors. As the temperature is lowered, the general trend is a loss of intensity in those bands associated with weakly (or non-) hydrogen-bonded components and a concomitant intensity increase in bands associated with the strongly hydrogen-bonded components. The changes in hydrogen-bonding interactions for bands between 1800 and 900 cm^{-1} agree with the change observed for the $\text{N}-\text{H}$ stretch (i.e., non-hydrogen-bonded $\nu(\text{N}-\text{H})$ at 3370 cm^{-1} decreasing and hydrogen-bonded $\nu(\text{N}-\text{H})$ at 3320 cm^{-1} increasing; data not shown). Table 2 lists the difference features observed between 1800 and 1000 cm^{-1} in Figure 2. Experiments performed on a pre-stretched sample show the same bands at the same

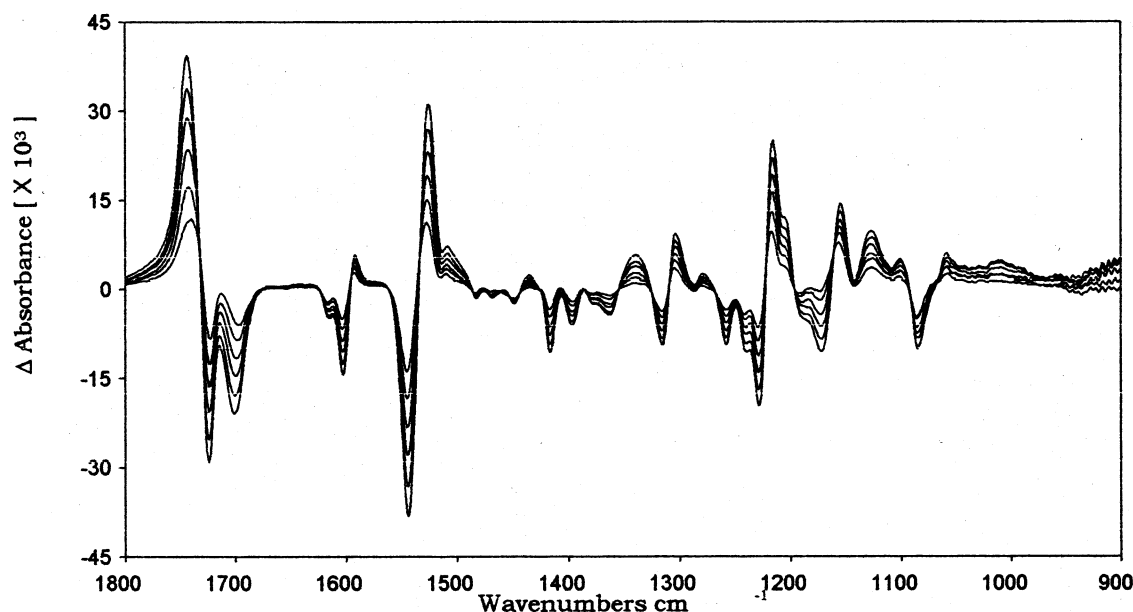


Figure 2. Static FTIR difference spectra ($1800\text{--}900\text{ cm}^{-1}$) as the temperature is lowered from 0 to $-30\text{ }^{\circ}\text{C}$ using the $25\text{ }^{\circ}\text{C}$ spectrum as the subtrahend.

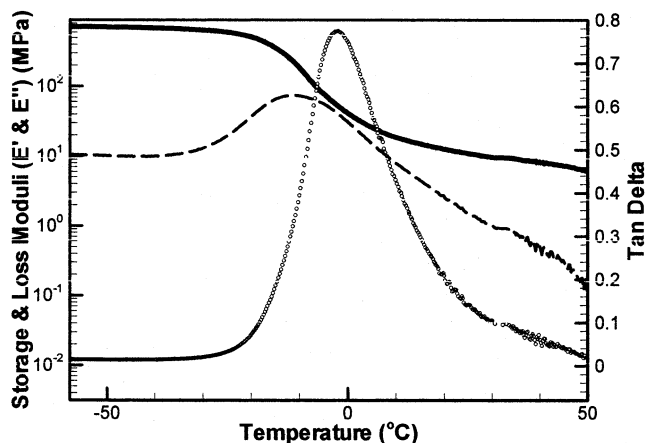


Figure 3. Dynamical mechanical analysis (DMA) data for solvent-cast thin film of the poly(ester urethane) that has been prretretched to 5 times its original length.

positions and demonstrate the same general changes with temperature. One noticeable difference is that the rate of change of the hydrogen-bonding component for the soft segment carbonyl band is slightly slower in the stretched sample.

Dynamic Mechanical Analysis (DMA). Dynamic mechanical analysis was utilized to monitor the macroscopic viscoelastic properties of Estane thin films under the same conditions as the DIRLD experiment. To allow for direct comparison with the DIRLD data, the sample was prestretched and the DMA experiment performed at 20 Hz. Storage modulus (E'), loss modulus (E''), and $\tan \delta$ are plotted in Figure 3. The loss modulus shows an α relaxation process centered near about -10°C . The details of this mechanical relaxation process are unknown but can be directly probed by the DIRLD experiment at -5°C . The storage modulus increases as the temperature is lowered, whereas $\tan \delta$ ($\tan \delta = E''/E'$) shows a maximum value at about -5°C , indicating that the DIRLD experiment at this temperature is performed near the soft segment glass transition in the stretched sample.

Variable Temperature DMA-FTIR Measurements. The in-phase and quadrature DIRLD data relate to the spectral responses in-phase with and 90° out-of-phase with the strain perturbation. For Estane, DIRLD data ($1800\text{--}900\text{ cm}^{-1}$) measured at $+25$ (room temperature), -5 , and -30°C , are shown in Figures 4, 5, and 6, respectively. To compare the differential responses of the transition moments of various functional groups, including their relative rates of orientation, the in-phase and quadrature spectra are also used to calculate the magnitude and phase spectra according to the following relationships.¹⁷

$$M(\bar{\nu}) = [I(\bar{\nu})^2 + Q(\bar{\nu})^2]^{1/2} \quad (1)$$

$$\Phi(\bar{\nu}) = \arctan[Q(\bar{\nu})/I(\bar{\nu})] \quad (2)$$

The peaks in the dynamic magnitude spectrum in Figure 7a indicate which functional groups produce a rheological response. The phase of each of these rheological responses at the corresponding frequency is given in the phase spectrum (Figure 7b). Although the phase spectrum shows numerous discontinuities (related to the phase boundaries in the tangent function), at each frequency corresponding to a band maximum in the dynamic magnitude spectrum, the corresponding phase

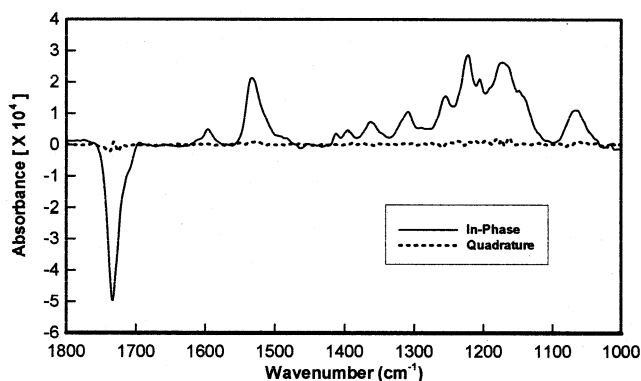


Figure 4. Dynamic infrared linear dichroism (DIRLD) spectra of Estane (parallel - perpendicular; in-phase (solid trace) and quadrature (broken trace); $1800\text{--}900\text{ cm}^{-1}$) measured at room temperature (ca. 25°C).

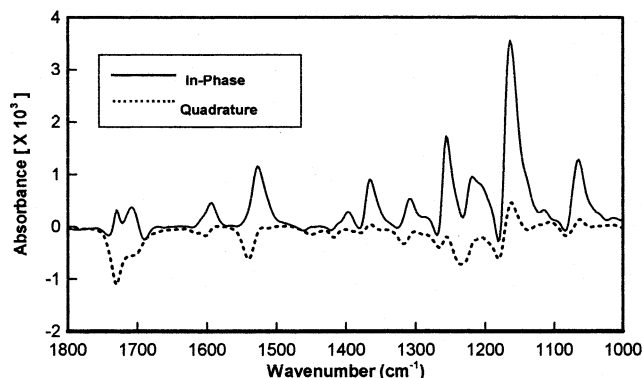


Figure 5. DIRLD spectra (in-phase, solid trace; quadrature, broken trace) of Estane measured at -5°C .

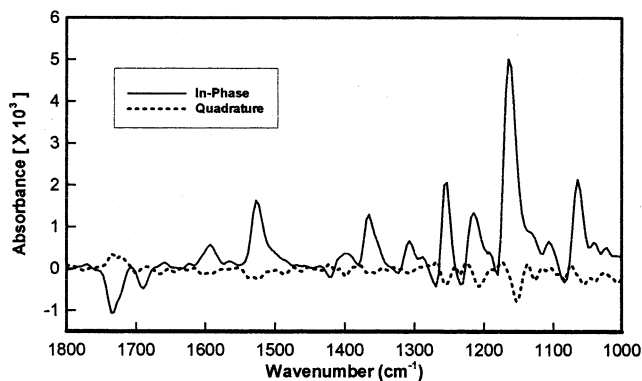


Figure 6. DIRLD data (plotted the same as Figures 4 and 5) of Estane measured at -30°C .

spectrum has a distinct (and significant) phase value. The phase values corresponding to the major bands shown in the magnitude spectrum are listed in Table 3.

Room Temperature DIRLD Spectra. The room temperature DIRLD data (Figure 4) demonstrate that the spectral (functional group) responses are predominantly in-phase with the strain perturbation. The difference spectra are in relative absorbance units (absorbance measured with parallel-polarized light, relative to the strain axis, minus absorbance measured with perpendicular-polarized light). The polarities of the in-phase spectrum, therefore, indicate the dynamic reorientation of specific functional groups. The spectra demonstrate that bands originating from stretching vibrations of the polymer backbone produce positive values in the differ-

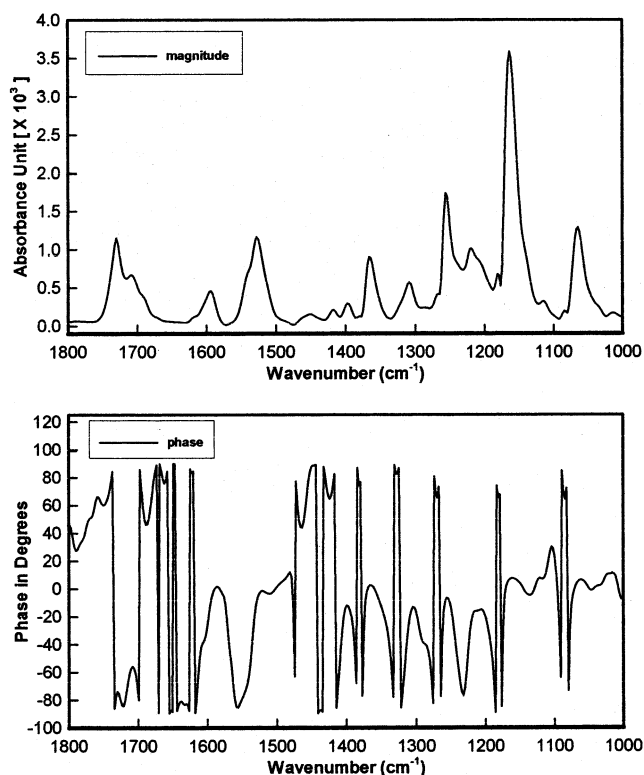


Figure 7. Dynamic magnitude and phase spectra calculated from the in-phase and quadrature DIRLD spectra of Estane at $-5\text{ }^{\circ}\text{C}$.

Table 3. DIRLD Phases of Selected Bands

| dynamic responses (cm^{-1}) | band assignments | segment origin | phase values (deg) |
|----------------------------------------|-----------------------------------|----------------|--------------------|
| 1730 | $\nu(\text{C}=\text{O})$ | soft | -76 |
| 1708 | $\nu(\text{C}=\text{O})$ | hard | -58 |
| 1690 | $\nu(\text{C}=\text{O})$ | hard | 50 |
| 1540 | amide II | hard | -40 |
| 1360 | $w(\text{CH}_2)$ | soft | -1 |
| 1256 | $\nu(\text{C}-\text{O}-\text{C})$ | soft | -4 |
| 1174 | $\nu(\text{C}-\text{O}-\text{C})$ | soft | 4 |
| 1074 | $\nu(\text{C}-\text{O}-\text{C})$ | hard/soft | 3 |

ence spectrum, indicating dynamic orientation of the transition moments *toward* the strain axis. Negative features, such as that for $\nu(\text{C}=\text{O})$, indicate dynamic rotation of these transition moments *away* from the strain axis. The most intense bands in the in-phase difference spectrum are from hard segment vibrations at 1733 ($\nu(\text{C}=\text{O})$), 1533 ($[\nu(\text{C}-\text{N}) + \delta(\text{N}-\text{H})]$), 1223 ($[\nu(\text{C}-\text{N}) + \delta(\text{N}-\text{H})]$), 1173 ($\nu(\text{C}-\text{O}-\text{C})$), and 1064 cm^{-1} ($\nu(\text{C}-\text{O}-\text{C})$).

$-5\text{ }^{\circ}\text{C}$ DIRLD Spectra. When the temperature is lowered to $-5\text{ }^{\circ}\text{C}$, the dynamic spectra (Figure 5) show significant changes compared to the room temperature results. The relative intensity in the in-phase dynamic spectrum is about an order of magnitude larger than the corresponding spectrum measured at room temperature. In addition to the signal magnitudes, other dramatic differences are also observed in the DIRLD spectra at $-5\text{ }^{\circ}\text{C}$ compared to the room temperature spectra. In the in-phase spectrum, the intensity of the carbonyl response is less relative to other bands, with two bands readily distinguished as positive features at 1730 and 1708 cm^{-1} . The variable temperature static FTIR data have been interpreted as indicating that these two bands are due to $\nu(\text{C}=\text{O})$ of hydrogen-bonded

ester groups and $\nu(\text{C}=\text{O})$ of hydrogen-bonded urethane groups, respectively.

In contrast to the room temperature results, the most intense bands in the $-5\text{ }^{\circ}\text{C}$ in-phase spectrum are due to soft segment vibrations at 1366 (CH_2 wag), 1256 ($\nu(\text{C}-\text{O}-\text{C})$, (CH_2 wag), 1164 ($\nu(\text{C}-\text{O}-\text{C})$), and 1064 cm^{-1} ($\nu(\text{C}-\text{O}-\text{C})$). The 1256, 1164, and 1064 cm^{-1} bands demonstrate less intense negative features on the high-frequency side of the intense positive bands. This type of bisignate response is typically seen for bands that undergo a frequency shift in the stress vs unstressed state, resulting in a derivative shape in the dichroic spectrum. Studies have shown that a shift of less than 1 cm^{-1} can result in an observable bisignate band.¹²

Also, in contrast to the room temperature data, significant intensity is observed in the quadrature (90° out-of-phase) $-5\text{ }^{\circ}\text{C}$ spectrum, indicating that some segmental responses are out-of-phase with the strain perturbation. Most of these out-of-phase bands are negative. In the carbonyl region, negative bands are observed at 1730 and 1706 cm^{-1} . The other strong negative bands are at 1541, 1234, and 1318 cm^{-1} ; all these bands are assigned the amide $[\nu(\text{C}-\text{N}) + \delta(\text{N}-\text{H})]$ vibrations. Another negative feature at 1181 cm^{-1} and the only positive band at 1162 cm^{-1} are assigned to a bisignate feature. Bisignate features are also observed for the $\nu(\text{C}-\text{O}-\text{C})$ bands of the soft segment at 1287/1256, 1181/1162, and 1082/1062 cm^{-1} . These bands are most pronounced in the in-phase spectrum with less magnitude in the quadrature spectrum.

$-30\text{ }^{\circ}\text{C}$ DIRLD Spectra. The $-30\text{ }^{\circ}\text{C}$ DIRLD data (Figure 6) show a larger in-phase response compared to the $-5\text{ }^{\circ}\text{C}$ data (Figure 5), particularly for the $\nu(\text{C}-\text{O}-\text{C})$ band near 1074 cm^{-1} . The in-phase spectrum at $-30\text{ }^{\circ}\text{C}$ is very similar to the $-5\text{ }^{\circ}\text{C}$ spectrum between 1650 and 900 cm^{-1} , with strong positive bands at 1593, 1527, 1365, 1254, 1215, 1165, and 1065 cm^{-1} . In contrast to the $-5\text{ }^{\circ}\text{C}$ spectrum, the carbonyl region at $-30\text{ }^{\circ}\text{C}$ shows two negative features at 1736 and 1690 cm^{-1} . The negative features between 1500 and 900 cm^{-1} are associated with bisignate bands of predominantly polymer backbone functional groups. Little signal is observed in the $-30\text{ }^{\circ}\text{C}$ quadrature spectrum, except for weak positive bands at 1736 and 1720 cm^{-1} and low-intensity negative bands at 1524, 1254, and 1153 cm^{-1} . The positive quadrature bands in the carbonyl region show the opposite polarity from those observed in the $-5\text{ }^{\circ}\text{C}$ quadrature spectrum.

$-5\text{ }^{\circ}\text{C}$ Dynamic Magnitude and Phase Spectra. The dynamic magnitude and phase spectra at $-5\text{ }^{\circ}\text{C}$ (Figure 7) assist in understanding the DIRLD data. The major dynamic responses can be classified into two categories: (1) backbone vibrations ($-\text{CH}_2-$ and $\text{C}-\text{O}-\text{C}$ stretching) and (2) vibrations of carbonyl and amide functional groups. The major responses from groups of the polymer backbone are from the soft segment groups. The hard segments do not show significant dynamic responses in the backbone region, but an intense hard segment response is noted for the amide vibrations at 1708 and 1540 cm^{-1} .

Discussion

The DSC data were utilized to provide insight into the temperature limits where the DIRLD measurements were performed. The extended rubbery region between -30 and $+40\text{ }^{\circ}\text{C}$ allows the material to be stretched

uniformly and studied by the DIRLD experiment. Below $-30\text{ }^{\circ}\text{C}$ the material becomes glassy and will craze or yield upon deformation. Above $40\text{ }^{\circ}\text{C}$, the disruption of the network structure weakens the material, and it will flow with stretching. The goal of this study is to probe the rheological responses at lowered temperatures and near the soft segment glass transition temperature to differentiate dynamic responses of functional groups in the hard or soft domains. With the lower temperatures, the numerous overlapping features in the infrared spectrum may be distinguished due to different reorientation response (rate and/or direction) to applied strain.

Hydrogen-bonding interactions play an important role in poly(ester urethanes), and the static FTIR spectra at lowered temperatures help to identify the band positions for the different hydrogen-bonding components. The urethane moiety is able to serve both as a hydrogen-bond donor and acceptor, while the ester groups can act only as acceptors. The static difference spectra measured between 0 and $-30\text{ }^{\circ}\text{C}$ provide a sensitive probe of the different hydrogen-bonding components. Probing this temperature regime using DIRLD can potentially provide insight into the distribution of hard segments in hard domains, at the interface of the two domains, and within urethane units dissolved in the soft domains. Since functional groups undergo selective reorientations induced by the small-amplitude oscillatory strain, each functional group (or more precisely the transition moment associated with the functional group) can respond distinctively to the applied strain in terms of rate and magnitude of response, and direction of reorientation, depending upon its specific local molecular environment, particularly with respect to "nonbonded" interactions, including hydrogen bonding.

The DMA data (on prestretched samples) show that as the temperature is lowered the soft segment glass transition occurs in the region between 0 and $-10\text{ }^{\circ}\text{C}$. The α relaxation process is evident, with a peak centered near $-10\text{ }^{\circ}\text{C}$ for the loss modulus. DIRLD experiments were performed at room temperature, near the soft segment T_g and in the area of the α relaxation process ($-5\text{ }^{\circ}\text{C}$), and below T_g at $-30\text{ }^{\circ}\text{C}$.

At room temperature, the DIRLD response is predominantly in-phase, with most of the intensity evident in bands originating from hard segment functional groups. This result is attributed to the fact that the samples were prestretched to between 5 and 6 times the original length prior to the DIRLD experiment. With this prestretching, the soft segments approach an orientation maximum and show greatly reduced response in the dynamic experiment.¹⁶ Most of the intensity in the dynamic spectrum is, therefore, from the hard segment bands. Taken together, the static and dynamic infrared linear dichroism results show the response of this polymer involves the soft segments providing the elasticity and reacting to the initial strain, while the hard segments add strength by reacting to the additional strain.¹⁶

As the temperature is lowered toward the T_g , polymers experience a broad phase transition. The free volume of the polymer decreases, and the mobility of the macromolecular chains changes. As the inter- and intramolecular contacts increase, so do the frictions inside the polymer. Comparison of the room temperature and $-5\text{ }^{\circ}\text{C}$ data can be related to several types of

microscopic (molecular) changes caused by the macroscopic deformation: (1) chain slippage, (2) bond and chain orientation, (3) bond stress, and (4) molecular interactions. At room temperature (above the T_g) the polymer has larger free volume and greater chain mobility (slippage). At $-5\text{ }^{\circ}\text{C}$, a larger DIRLD signal is observed, indicating a large orientational effect rather than chain slippage. In addition, for most backbone functional groups, bond stress occurs, giving rise to slight frequency shifts resulting in bisignate bands in the DIRLD spectra.

Chase and Ikeda have noted that the intensity in the in-phase dynamic dichroism scales with the modulus.^{18,19} As the temperature is lowered, the stiffness of the polymer increases and the modulus increases. The DMA results show an increase in modulus with the lower temperatures, and the in-phase spectrum at $-5\text{ }^{\circ}\text{C}$ shows greater ΔA values compared to room temperature.

The in-phase DIRLD spectrum at $-5\text{ }^{\circ}\text{C}$ demonstrates reorientation of transition moments of functional groups predominantly toward the deformation direction; only very slight negative features are observed. As the temperature approaches the soft segment T_g , the greatest intensity in the dynamic spectrum originates from the soft segment functional groups, which are most affected as the temperature approaches T_g . The in-phase spectrum corresponds to the instantaneous dichroism observed when the *magnitude* of the applied strain is a maximum. The greatest elastic response at $-5\text{ }^{\circ}\text{C}$ is, therefore, from soft segment function groups. The most intense features in the in-phase spectrum are the 1164 and 1256 cm^{-1} bands, indicating that the ester C—O—C segments respond most readily and most extensively to the directional strain. The positive sign of these bands would indicate that near T_g these transitional dipoles are orienting toward the strain axis.

With the lower temperature, the polymer becomes more rigid, thereby altering the response of function groups. This fact is manifest in significant quadrature intensity. The quadrature spectrum corresponds to the dichroism observed when the *rate* of the dynamic strain is a maximum, thus demonstrating viscous response. The quadrature spectrum at $-5\text{ }^{\circ}\text{C}$ indicates considerable out-of-phase response, primarily in the bands of hard segment functional groups. These bands are associated with the hydrogen-bonded component of these vibrations. The hydrogen-bonded groups (most noticeably $[\nu(\text{C—N}) + \delta(\text{N—H})]$, $\nu(\text{C=O})$, and phenyl ring ($\text{C=C}) + \delta(\text{N—H})$ bands) of the hard segments are responding out-of-phase. However, since the negative sign of the phase indicated by the negative quadrature signal does not distinguish between the second and fourth quadrants, orientation information from the quadrature signal remains ambiguous in the absence of a more detailed temperature study. Nevertheless, the differences in phase response between different functional groups and the changes in these relationships as a function of temperature are unmistakable.

Bisignate bands typically indicate stress-induced frequency shifts, but other factors can give rise to these features, including changes in intensity, band shape, and/or bandwidth. Hydrogen-bonding interactions can also affect these features of the IR bands.¹⁹ At $-5\text{ }^{\circ}\text{C}$, many of these bisignate features in the dynamic spectra correspond to hydrogen-bonding pairs, with the reorientation of the hydrogen-bonded component and that

of the free component being distinguished. As the temperature is lowered, the different responses for the same functional group demonstrate the differences in the microenvironment, in this case a strongly hydrogen-bonded group vs a weakly (or non-) hydrogen-bonded group.

In the $-5\text{ }^{\circ}\text{C}$ DIRLD data, the carbonyl stretching region demonstrates a large out-of-phase component, with the dynamic response clearly split into two distinct features. The in-phase signal also demonstrates two distinct responses. This observation shows that responses from urethane and ester $\nu(\text{C}=\text{O})$ can be distinguished at $-5\text{ }^{\circ}\text{C}$. The orientation signal of $\nu(\text{C}=\text{O})$ is relatively weak compared to the other bands, even though it is strong in the static FTIR spectrum and the in-phase DIRLD spectrum at room temperature. This implies that the lowering of the temperature significantly changes the mobility of the $\text{C}=\text{O}$ groups.

No significant response is observed at $-5\text{ }^{\circ}\text{C}$ for the free $\nu(\text{C}=\text{O})$ component, in contrast to the room temperature data, which show a large orientation away from the stretch direction for all carbonyl bands. The in-phase spectrum shows that some set of hydrogen-bonded carbonyl groups of both segments are responding in-phase and in a parallel direction, while the quadrature spectrum indicates that some portion of same groups are responding out of phase. These data show that different populations of the same functional group have different microenvironments that can be distinguished at $-5\text{ }^{\circ}\text{C}$. The hydrogen-bonded carbonyl of the urethane can reside within the hard domains surrounded by several urethane units or in closer contact with several soft domains (on the surface of the hard domains or within the soft domains). Similarly, the polyester carbonyl can be hydrogen-bonded to the urethane $\text{N}-\text{H}$ at the surface of the hard domains or to a urethane segment within the soft domains. The carbonyls in these different environments respond differently to the applied stress at lower temperatures, giving rise to different signals in the dynamic experiment. For the in-phase spectra, the sign changes in the carbonyl region from negative to positive to negative in the 25, -5 , and $-30\text{ }^{\circ}\text{C}$ spectra. This abrupt change in sign occurs when the temperature passes through the α relaxation, reflecting the overall orientation direction changes for the carbonyls. The dynamic dichroism near the α relaxation reflects the molecular-level orientation responses coupled to the perturbation of the overall polymer morphology.²⁰

The phase spectrum at $-5\text{ }^{\circ}\text{C}$ indicates that all of the backbone vibrations have phase values near zero degrees, indicating that their motions are in-phase with the dynamic strain. The ester carbonyl band at 1730 cm^{-1} and the amide vibrations at 1708 and 1540 cm^{-1} have large negative dynamic response phases. The corresponding transition moments of these functional groups are responding out-of-phase with or lagging behind the dynamic strain. An exception is the response phase at 1690 cm^{-1} that has a phase value of 50° . The in-phase spectrum in Figure 5 shows a bisignate shape associated with this feature. No $\nu(\text{C}=\text{O})$ band or component of an infrared band has been observed in the static spectrum of Estane at this frequency. The phase difference between 1708 and 1690 cm^{-1} is therefore assigned to a frequency shift.

The phase shift of the hard segment carbonyl is greater in the in-phase channel, while the orientation

is greater in the quadrature channel. The shift is to higher energy when the polymer is strained, which is opposite to what has been observed previously when the frequency shift is due to the deformation of the bond angle and bond length.¹⁴ This type of deformation often weakens the bond and causes a shift to a lower energy. The observed shift in the current data is more likely due to changes in the hydrogen-bonding interactions when the polymer is strained.

The comparison of in-phase and quadrature data for the hard segment $[\nu(\text{C}-\text{N}) + \delta(\text{N}-\text{H})]$ vibrations shows the same behavior. The in-phase spectrum demonstrates parallel reorientation of the non-hydrogen-bonded components at 1527 , 1309 , and 1219 cm^{-1} . The quadrature spectrum shows out-of-phase response of the hydrogen-bonded components of these same vibrations at 1541 , 1318 , and 1234 cm^{-1} . The free components demonstrate an elastic response, while hydrogen-bonded groups show a viscous response.

At $-30\text{ }^{\circ}\text{C}$, the polymer is nearing free volume collapse with significantly reduced chain mobility. The $-30\text{ }^{\circ}\text{C}$ DIRLD data demonstrate that the dynamic spectral changes are primarily in-phase with the strain perturbation. The $\nu(\text{C}=\text{O})$ orientation is still observable but with a smaller magnitude, and the responses from the urethane and the ester carbonyls are separated into two features. The carbonyl groups cannot orient as freely in response to the deformation.

The major difference between the spectra at -5 and $-30\text{ }^{\circ}\text{C}$ is the response in the carbonyl region. The predominant contributor to the in-phase spectrum at $-30\text{ }^{\circ}\text{C}$ is the perpendicular orientation of the non-hydrogen-bonded $\nu(\text{C}=\text{O})$. A negative feature at 1690 cm^{-1} is again associated with the $1708/1690\text{ cm}^{-1}$ bisignate feature. In the quadrature spectrum at $-30\text{ }^{\circ}\text{C}$, less intensity is observed relative to the $-5\text{ }^{\circ}\text{C}$ spectrum, indicating less out-of-phase (viscous) response. The negative features do not correlate to hydrogen-bonded components as was observed at $-5\text{ }^{\circ}\text{C}$. In the carbonyl region, weak responses of the non-hydrogen-bonded carbonyl groups and hydrogen-bonded carbonyls of the soft segment are evident. The non-hydrogen-bonded carbonyl response at 1736 cm^{-1} can be from either hard or soft domains.

Conclusions

The increase of the dynamic orientation signal magnitude as the temperature is lowered indicates that the macroscopic deformation of the polymer at higher temperatures is primarily due to the random flow of the molecular chains rather than orientation. Approaching T_g , more alignment in the transition moments of soft segment functional groups occurs in response to the imposed strain. The changes in chain mobility also lead to the emergence of DIRLD bisignate band shapes in the backbone vibrational region of the polyester segment. These bipolar bands indicate changes in the strength of the vibrational dipoles, demonstrating stress of the molecular bonds and/or change of the inter- and intramolecular interactions due to the loss of free volume and molecular mobility.

The changes in the carbonyl region as a function of temperature in both the in-phase and quadrature spectra are complex but reveal the different responses of the various carbonyl functional groups in the polymer. The urethane and ester carbonyl groups, with their different interactions and microenvironments, are not

observed by other experimental approaches, nor are they evident in the static FTIR spectra. The dynamic dichroic data at -5°C show significant intensities in the quadrature channel. Phase analysis indicates that the changes of the amide bands lag behind those of the backbone bands. These changes demonstrate a temperature dependency related to the hydrogen-bonding interactions. At room temperature, the collective contributions of these infrared bands are not distinguished, resulting in an intense negative band in the in-phase DIRLD spectrum and no quadrature signal. As the temperature is lowered, the responses of the carbonyls are altered, and the different components are observed and differentiated.

Acknowledgment. Part of this work was performed at Los Alamos National Laboratory under the auspices of the U.S. Department of Energy under contract with the University of California W-7405-ENG-35. The authors acknowledge the support of the Laboratory Directed Research and Development Program, the Technology Partnership Program, Enhanced Surveillance Program at Los Alamos for support of this work. D.G.T. also thanks the Director's Funded Postdoctoral Program at Los Alamos for support. R.A.P acknowledges support from the Lord Foundation of North Carolina, Bruker Optics, and Duke University.

References and Notes

- (1) Siesler, H. W.; Holland-Moritz, K. *Infrared and Raman Spectroscopy of Polymers*; Marcel Dekker: New York, 1980.
- (2) Fawcett, A. H. *Polymer Spectroscopy*; John Wiley & Sons Ltd.: Chichester, 1996.
- (3) Elias, H. *Macromolecules*, 2nd ed.; Plenum Press: New York, 1984.
- (4) Noda, I.; Dowrey, A. E.; Marcott, C. *Appl. Spectrosc.* **1988**, *42*, 203–216.
- (5) Chase, B.; Ikeda, R. *Appl. Spectrosc.* **1993**, *47*, 1350–1353.
- (6) Palmer, R. A.; Smith, M. J.; Manning, C. J.; Chao, J. L.; Boccara, A. C.; Fournier, D. *Photoacoustic and Photothermal Phenomena*; Proceedings of the 5th International Topical Meeting, Heidelberg, Germany, July 1987; Hess, P., Pelzl, J., Eds.; Springer Series in Optical Sciences; Springer-Verlag: New York, 1988; Vol. 61.
- (7) Smith, M. J.; Manning, C. J.; Palmer, R. A.; Chao, J. L. *Appl. Spectrosc.* **1988**, *42*, 546–555.
- (8) Palmer, R. A. *Spectroscopy* **1993**, *2*, 26–36.
- (9) Palmer, R. A.; Manning, C. J.; Chao, J. L.; Noda, I.; Dowrey, A. E.; Marcott, C. *Appl. Spectrosc.* **1991**, *45*, 12–17.
- (10) Gregoriou, V. G.; Noda, I.; Dowrey, A. E.; Marcott, C.; Chao, J. L.; Palmer, R. A. *J. Polym. Sci., Part B: Polym. Phys.* **1993**, *31*, 1769–1777.
- (11) Palmer, R. A.; Gregoriou, V. G.; Fuji, A.; Jiang, E. Y.; Plunkett, S. E.; Connors, L. M.; Boccara, S.; Chao, J. L. In *Multidimensional Spectroscopy in Polymers*; ACS Symposium Series 598; Urban, M. W., Provder, T., Eds.; American Chemical Society: Washington, DC, 1995; pp 99–116.
- (12) Budevskaya, B. O.; Manning, C. J.; Griffiths, P. R.; Roginski, R. T. *Appl. Spectrosc.* **1993**, *47*, 1843–1851.
- (13) Ingemey, R. A.; Strohe, G.; Veeman, W. S. *Appl. Spectrosc.* **1996**, *50*, 1360–1365.
- (14) Wang, H.; Palmer, R. A.; Manning, C. J. *Appl. Spectrosc.* **1997**, *51*, 1245–1250.
- (15) Wang, H.; Graff, D. K.; Schoonover, J. R.; Palmer, R. A. *Appl. Spectrosc.* **1999**, *53*, 687–696.
- (16) Graff, D. K.; Wang, H.; Palmer, R. A.; Schoonover, J. R. *Macromolecules* **1999**, *32*, 7147–7155.
- (17) Jiang, E. Y.; Palmer, R. A. *Anal. Chem.* **1997**, *69*, 1931–1935.
- (18) Chase, D. B.; Ikeda, R. M. *Appl. Spectrosc.* **1999**, *53*, 17–21.
- (19) Chase, D. B.; Ikeda, R. M. *Macromol. Symp.* **1999**, *141*, 217–226.
- (20) Noda, I.; Dowrey, A. E.; Marcott, C. *Fourier Transform Infrared Characterization of Polymers*; Ishida, H., Ed.; Plenum: New York, 1987; pp 33–59.

MA012135A